X-ray Image Subtraction by Digital Means

Abstract: A conventional method of removing unwanted background information from radiographic images is to use photographic techniques. An alternative approach is the digital processing of x-ray difference images. This approach offers the advantage over photographic methods in that it permits the performance of nonlinear operations, such as compensation for film characteristics, thus offering greater flexibility in the presentation of x-ray images and greater reliability in their interpretation. This paper describes the features and implementation of a new digital approach and presents experimental results obtained from processing two sets of angiograms.

1. Introduction

An important medical radiographic image-processing technique is known as *subtraction* [1]. It is essentially a method of removing unwanted background information from an x-ray image. The processing involves two radiographic exposures taken before and after a suitable contrast agent or dye has been introduced into the specimen of interest. The desired result is to increase the visibility of image features by emphasizing the presence of the contrast agent through the subtraction of background detail. Background information occurs as a result of x-ray absorbing material that exists in the specimen being studied.

In a radiographic system, the x-ray energy available for exposure of the film is attenuated exponentially as it passes through the specimen. This exposure energy is a two-dimensional function, which can be written as

$$E(x, y) = E_0 \exp \left[-\beta(x, y)\right],$$

where E_0 is the energy incident on the specimen (assumed uniformly distributed) and $\beta(x,y)$ represents the attenuating effects of the materials in the specimen. Absorption is here considered to be the dominant attenuation process. The function $\beta(x,y)$, herein called the attenuation projection, is determined by the composite effect of the several absorbing materials present in a specimen. Subtraction normally attempts to remove all effects except that of a prepared contrast agent.

In the work reported here, registration alignment of two images is required, but relative geometric distortion between the images is not large enough to warrant correction. The application of digital techniques to x-ray image enhancement, where geometric changes involving relatively large features occur between the times at which the two exposures were made, has been reported previously [2].

2. Basic relations and assumptions

The type of experimental arrangement we are considering is depicted in Fig. 1. There is a source of x-rays whose output beam is collimated onto a specimen. As the x-rays pass through the specimen, they are attenuated exponentially by the local variations in the material attenuation characteristics, which are assumed to be predominantly the result of absorption phenomena. A reduced x-ray strength is available for exposure of a closely positioned x-ray film. For much of medical radiographic work, the film is positioned within intensifying screens so that light energy (after conversion from x-ray energy) is the primary means of film exposure.

As suggested by Fig. 1, a small amount of magnification (typically in the range from $1.02\times$ to $1.2\times$, depending on the type of radiographic examination) is normally introduced as a result of a separation between the specimen and recording medium. This effect and geometric unsharpness (penumbra) caused by the combination of source size and magnification are not included in the following discussions in order to simplify the presentation.

The subtraction technique is conveniently implemented with photographic methods. This is the current practice. By restricting exposure to the so-called linear portions of the sensitometric curves of x-ray and photo-

graphic films, it is possible to prepare a difference image that is a facsimile of the original x-ray image with the background removed.

With digital image processing, however, one is not limited to the linear portions of the film characteristic curves in order to achieve high-fidelity results. Moreover, with knowledge of the x-ray film characteristic curve, it is possible to extract exposure variations normally suppressed because they occur at relatively high or low levels on the sensitometric curve. Thus, one is able to make use of a greater x-ray exposure range.

It is apparent that the digital approach to subtraction should provide convenient access to quantitative difference information. Furthermore, it is possible to assign values to the attenuation projection, $\beta(x, y)$, and its constituents, and to perform operations that are not feasible with photographic or optical means.

Finally, digital processing offers flexibility in the presentation of the images resulting from digital subtraction. The attenuation projection can be displayed directly in terms of transmittance or in its exponentiated form (similar to photographic method output). Alternatively, the display can be adjusted to compensate for the eye response. Another important reason for digital processing is that the effective contrast in the resultant image can be automatically and spatially varied to further enhance the display.

We assume that the attenuation coefficients of the absorbing materials are frequency independent over the range of x-ray energy available. This is a reasonable approximation in many diagnostic situations. However, the following developments can be expected to show some error in certain diagnostic situations, e.g., soft-tissue absorption of low-energy photons.

Consider an inhomogeneous specimen (of thickness not exceeding L) consisting of various absorbing materials. Let $\alpha(x,y,z)$ be the value of the linear attenuation coefficient at point (x,y,z) in the object. In general, the function $\alpha(x,y,z)$ includes the effects of the three-dimensional geometric distribution of the constituent materials present. Since $\alpha(x,y,z)$ is based upon the linear attenuation coefficients existing in the specimen, it follows (assuming propagation in the z-direction) that the energy available to the recording medium is given by

$$E(x,y) = E_0 \exp \left[-\int_0^L \alpha(x,y,z) dz \right],$$

where E_0 is the spatially uniform energy incident on the specimen.

It is apparent that, for the assumptions stated above, the previously introduced radiographic attenuation projection is given by

$$\beta(x,y) = \int_0^L \alpha(x,y,z) dz.$$

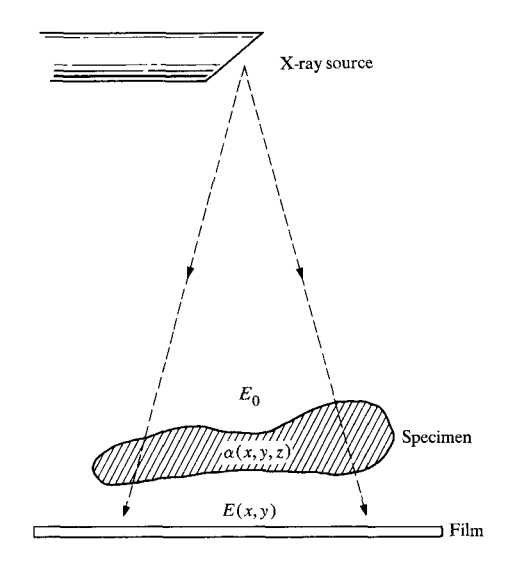


Figure 1 Radiographic configuration.

This function has quantitative significance. For example, we can say that it represents

- the sum of the products of the linear attenuation coefficients and the respective thicknesses of the absorbing materials, or
- 2. the sum of the products of the mass absorption coefficients and the mass per unit area.

The attenuation projection is a two-dimensional representation of the amount and type of material encountered by the x-rays as they pass through the specimen.

A representative x-ray film (Dupont Cronex 2DC) characteristic curve is shown in Fig. 2. The extremes of the curve have the effect of suppressing the measured density or transmittance variations. Even in the so-called linear region of the curve, the slope, or γ , shows some change. With prior knowledge of the x-ray film characteristic curve, it is possible to convert measured transmittance or density values to relative exposure. As a result, it is possible that signal variations that reside at extreme levels of exposure can be restored through computer processing.

In mathematical terms, if the background attenuation projection is $\beta_b(x, y)$ and the projection after introduction of a contrast agent is $\beta_b(x, y) + \beta(x, y)$, then the difference projection is

$$\beta(x, y) = \ln \left[E_{\mathrm{b}}(x, y) / E_{\mathrm{a}}(x, y) \right],$$

where $E_b(x, y)$ and $E_a(x, y)$ are the relative exposures before and after introduction of dye [3]. This relationship involving the ratio of the exposure energies is general and basic to the importance of subtraction.

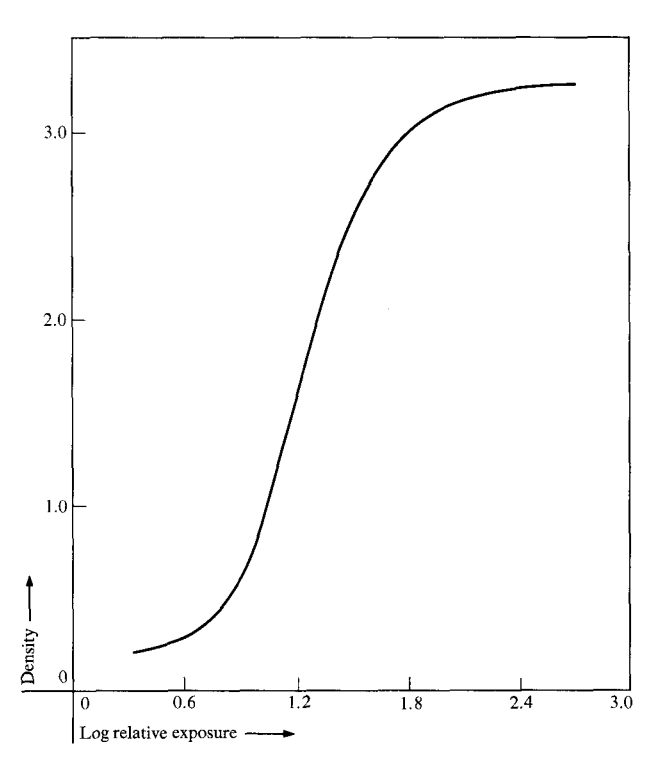


Figure 2 Form of typical characteristic curve for x-ray film.

3. Photographic subtraction

Because radiographic subtraction is normally accomplished with photographic techniques, it is useful to understand this method as a basis for reference and comparison with the digital image processing approach.

Briefly, the typical photographic approach consists of the following steps. A negative transparency or mask is made from the x-ray film obtained before the contrast agent is introduced. This mask is superimposed (with appropriate registration) upon the film obtained after the injection of contrast material, and the combination of images is viewed by a radiologist. The scene available is, ideally, the desired difference image with all of the background removed. The result is readily recorded as a negative transparency. An additional photographic processing step can then provide a positive transparency, if desired.

The foregoing description can be conveniently represented mathematically since the linear region of the film characteristic is a necessary ingredient to the argument. In this region, the relation between optical transmittance, T, and exposure, E, is $T=10^{D_0}\,E^{-\gamma}$, where D_0 and γ are constants of the film and its processing. This general relation applies to both photographic and x-ray exposures although the constants would be different.

The x-ray energies available for exposure before and after introduction of a contrast agent, respectively, are given by

$$E_{\rm b}(x,y) = E_{\rm o} \exp \left[-\beta_{\rm b}(x,y)\right]$$

and

$$E_{a}(x, y) = E_{0} \exp \left[-\beta_{b}(x, y) - \beta(x, y)\right].$$

 $\beta_{\rm b}(x,y)$ is the background attenuation projection and the primary function of interest, $\beta(x,y)$, is the attenuation projection due to introduction of the dye. The exposure energy, $E_{\rm o}$, incident on the specimen is assumed to be spatially uniform. Also, in this discussion, scattering and diffraction are neglected.

The resulting transmittances of the two x-ray images are given by

$$T_{\rm b}(x,y) = K_{\rm t} \exp \left[\gamma_{\rm x} \beta_{\rm b}(x,y) \right]$$

and

$$T_{a}(x, y) = K_{1} \exp \left[\gamma_{x} \beta_{b}(x, y) + \gamma_{x} \beta(x, y)\right]$$
$$= T_{b}(x, y) \exp \left[\gamma_{x} \beta(x, y)\right],$$

where γ_x refers to the slope of the x-ray film sensitometric curve, and K_1 is a constant. (In the following, all K's are constants.)

The energy available for exposure of the mask associated with $T_{\rm b}(x,y)$ is

$$E_{\rm bm}(x, y) = K_{\rm p} T_{\rm b}(x, y) ;$$

so the transmittance of the mask can be written as

$$T_{\rm bm}(x,y) = K_3 T_{\rm b}(x,y)^{-\gamma_{\rm m}},$$

where γ_m need not necessarily be the same as γ_x . The following development will demonstrate that, regardless of the value of γ_x , the optimum value for γ_m is unity. Cascading of the "before" mask and "after" transparency permits an exposure energy of

$$E_{d}(x, y) = K_{4} T_{bm}(x, y) T_{a}(x, y)$$

$$= K_{5} T_{b}(x, y)^{(1-\gamma_{m})} \exp \left[\gamma_{x} \beta(x, y)\right];$$

so the difference image print will have the form

$$T_{\rm d}(x,y) = K_6 T_{\rm b}(x,y)^{-(1-\gamma_{\rm m})\gamma_{\rm d}} \exp \left[-\gamma_{\rm x} \gamma_{\rm d} \beta(x,y)\right],$$

where, in principle, γ_d need not be the same as γ_m . It is apparent that if γ_m is chosen to be unity, the difference becomes

$$T_{d}(x, y) = K_{6} \exp \left[-\gamma_{x} \gamma_{d} \beta(x, y)\right]$$

and the effect of the background is now removed. In fact, the transmittance becomes functionally "perfect" if a positive transparency is made, e.g.,

$$T_{\rm dp}(x,y) = K_7 \exp \left[\gamma_{\rm x} \gamma_{\rm d} \gamma_{\rm dp} \beta(x,y) \right],$$

with the product $\gamma_d \gamma_{dp} = 1$. We see that the relation is identical to the original transmittance relation had there been no background, $\beta_b(x, y)$, present.

As indicated, the foregoing analysis is restricted to the linear portion of the film sensitometric curve. Although the analysis does not lend itself to easy mathematical treatment, it is possible to improve the photographic result by utilization of a modified technique known as second-order subtraction [4]. Two masks must be created in this case. The benefits of second-order subtraction are partial correction for nonlinearity of the curve and some amount of compensation for those cases in which the mask gamma, γ_m , is not unity.

4. Output presentation

Digital processing lends itself to flexibility in output presentation. As indicated earlier, the effective attenuation projection can be computed from the exposure functions, which in turn are translated from measured transmittance image functions. There are many ways to present the results of digital subtraction. One means of displaying the effective attenuation projection as an image is with a transmittance variation that is directly proportional to $\beta(x, y)$, e.g.,

$$T_{\rm d}(x,y) = K_8 \beta(x,y) .$$

To reconstruct a "clean" x-ray exposure, the exponential dependence can be restored so that the image becomes

$$T_{d}(x, y) = K_{g} \exp \left[\gamma_{c}\beta(x, y)\right]$$
$$= K_{10} \left[E_{b}(x, y) / E_{a}(x, y)\right]^{\gamma_{c}},$$

where the value of γ_c can be selected to be the same as or different from that of the original x-ray film. Thus, to the extent that the recording film dynamic range permits, contrast enhancement is possible. In any case, by comparison with the results of the preceding section it is apparent that this particular output formulation agrees structurally with the results of photographic subtraction. The photographic theory presented earlier was valid only over the linear region of the characteristic curve, while the method of digital subtraction and presentation indicated in the above equation is not restricted in this important aspect. Furthermore, artificially generated "positive" or "negative" displays can be generated by the proper choice of sign for γ_c .

For these reasons, the majority of results shown in our experimental investigation utilize this formulation. However, the quantity γ_c will henceforth be called a contrast parameter since the particular recording devices employed were operated in a manner such that there did not exist a 1:1 relation between computed transmittance and recorded transmittance.

Finally, one can attempt to achieve eye-response compensation with the display. A certain amount of controversy exists as to whether this response tends to be logarithmic (in which case the preceding display technique involving exponentiation is already applicable), or to follow a power law [5]. For the latter case, an applicable form of the transmittance is

$$T_{\rm d}(x,y) = K_{11}\beta(x,y)^k,$$

in which k is chosen to be about 3.

The normal method of implementation of the previously described exponentiation technique is to pick fixed values of the contrast parameter, γ_c , and to compute the corresponding transmittance image. However, it frequently happens that the value of γ_c , which is optimum in regions with minimal background, is not suitable for regions of high background. This situation can occur, for example, when the dynamic range of the recording medium is inadequate. To improve visualization, it is desirable to vary the contrast parameter spatially and, consequently, to vary the contrast as a function of background intensity in different regions. Since the exposure function of the "before" image is a measure of the background, it is used as a control function to set the variable contrast parameter. An example of one such implementation is given as

$$\gamma_{\rm e}(x, y) = K_{12} + K_{13} [E_{\rm b}(x, y)]^{-1},$$

where the K's are constants chosen to vary γ_c over the desired range. This type of data-dependent contrast enhancement requires an additional processing step but has the distinct advantage of providing automatic contrast adjustments.

5. Implementation

A representative flowchart for the operations performed in our implementation of digital subtraction is shown in Fig. 3. The facilities that were available to this investigation are shown in the block diagram of Fig. 4. The input-output operations were usually accomplished with image processing equipment attached to an IBM 1800 process controller [6]. Interactive processing on extractions of the full-size images was done on a time-sharing computer system (TSS/360) using a special image processing supervisory program developed by R. Bakis. Temporary results obtained interactively were transmitted to the 1800 for TV display. Digital processing of the full-size images was accomplished with an IBM System/360 Model 91.

One means of image input was an image dissector TV camera under control of the 1800. This system has a special dc light box that provides illumination for scanning x-rays as large as 41 cm by 51 cm. The 2.5-cm circular photocathode and 25- μ m aperture permit a maximum useful circular field size of 1000 pixels in diameter. The amplitude noise level was measured to be 1% at full amplitude. However, at the time we were using this sys-

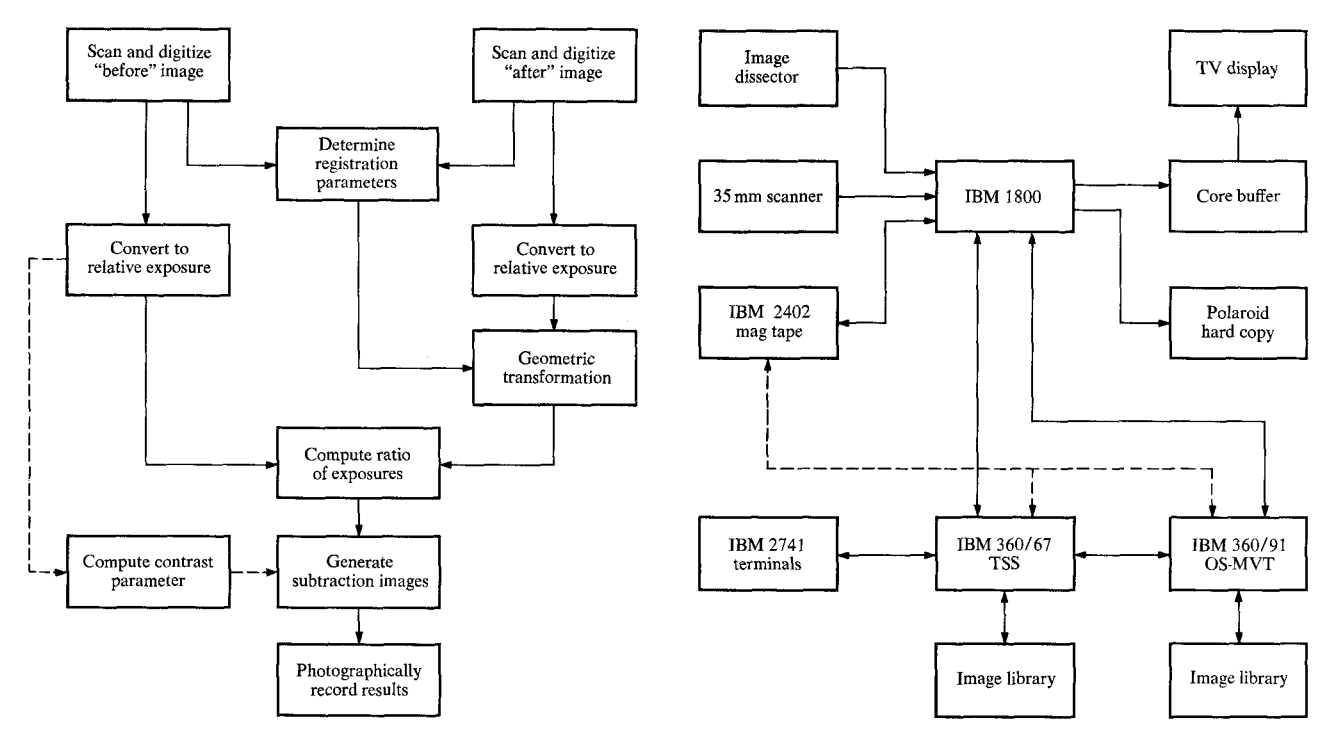


Figure 3 Steps in digital subtraction.

Figure 4 Facilities for digital processing of x-ray images.

tem for scanning the difference images, the deflection system was producing an unwanted "hum" that resulted in a noticeable degradation in signal-to-noise ratio.

Because of the image dissector camera deflection problem, an alternative input method was also employed. This was the use of an Optronics International, Inc. System P-1000 Photoscan mechanical drum scanner. The particular model used had an available field of about 12.7 cm by 17.8 cm with the overall width of a transparency restricted to 18.7 cm.

All images were raster scanned. The data obtained from the Optronics scanner were recorded in terms of optical density. When the image dissector was used, non-uniformities in the light box illumination and photocathode sensitivity required normalization; a reference scan was first taken with the x-ray film removed and the image scan was later divided digitally by the reference scan to obtain an image meaningful in terms of optical transmittance.

All scanned images were recorded on digital magnetic tapes that were hand-carried to the Model 91 for further processing. On this system, the images were converted to transmittance representations and stored as direct-access data sets on an IBM 2316 Disk Pack. The size of the images stored and processed on the Model 91 was 1024×1024 pixels.

Unfortunately, only coarse registration alignment was cone on the images prior to the original scanning process. As a result, it was somewhat difficult to determine the registration parameters after the images were spatially digitized. Also, automatic digital registration techniques (e.g., [7]) were not implemented since this was to be a short-term exploration. Trial and error registration processing on the full-size image was prohibitive in terms of both system resources and turn-around time.

The course chosen for registration was to extract 256×256 pixel portions from the 1024×1024 pixel full-size images, store the extractions on the TSS/360 system and process these images in an interactive manner. The extractions could be of the same spatial resolution (by using a selected portion of the original image; e.g., a corner) or sampled versions of the full image. Unless unusually distinct features were available, the later type of extraction proved more convenient.

Coarse registration was accomplished by two methods. The first method involved direct visual comparison of the geometrically transformed image (which was arbitrarily chosen to be the "after" image) with the other image. The comparisons were made by viewing split-screen TV images or Polaroid prints. The locations of common features were compared and used to predict the next trial parameters. An alternative method proved

useful when particularly distinct common features were available. In this case, gray-level slicing thresholds were chosen to outline the features and the resulting binary images were directly subtracted to produce a resultant image. Examples of the TV monitor presentations of the images obtained with this approach are shown in Fig. 5. The picture in Fig. 5(a) illustrates the situation prior to registration, while the picture in Fig. 5(b) gives an example of an image that is close to proper alignment.

Fine registration alignment was also done interactively. The method of generating the difference radiographs is such that, neglecting physical movement, at every corresponding point the transmittance of the "after" image should always exceed that of the "before" image. Subtraction of a properly aligned set of difference images should produce a unipolar resultant image. This principle was made use of by performing the subtraction on the gray-scale transmittance images, examining the resultant histogram and then comparing it to those of other trials. Minimization of the inevitable discrepancies at the 0.1% and 1% points of the cumulative distribution were the best indicators of proper registration.

After the registration parameters were determined, processing of the full-size images stored in the Model 91 was performed. The transmittance representations were converted to relative exposure representations based upon linear interpolation of a 28-point approximation to the x-ray film sensitometric curve. Points were taken from a standard curve for Dupont Cronex 2DC film, although an actual calibration using a gray-scale wedge would have assured more accurate results.

After conversion of the images to relative exposure representations, the previously determined registration parameters were applied to geometrically transform the "after" image by the proper amount. This step tends to require large amounts of computing resources if rotation is needed. Because of core storage limitations and job priority considerations, only a fraction of the image could be manipulated at any one time. Although other arrangements were possible, we used image slices corresponding to $\frac{1}{32}$ th of the total image height. As a result, execution of a program written in FORTRAN to perform a 5° rotation with linear interpolation between the four nearest neighbors required less than 5 minutes of CPU time (the system contained 382K bytes of core storage), but more than 1 hour of system time to accomplish the disk I/O operations. Fortunately, this step was a "one-time" operation for each set of images.

The next processing step was to divide the geometrically transformed "before" exposure image by the "after" exposure representation. This ratio was an intermediate result that was also stored on disk to avoid repetition of the prior geometric transformation. The ratio representation was used to generate a number of "posi-





Figure 5 Images photographed from TV screen. (a) Before registration; (b) after registration.

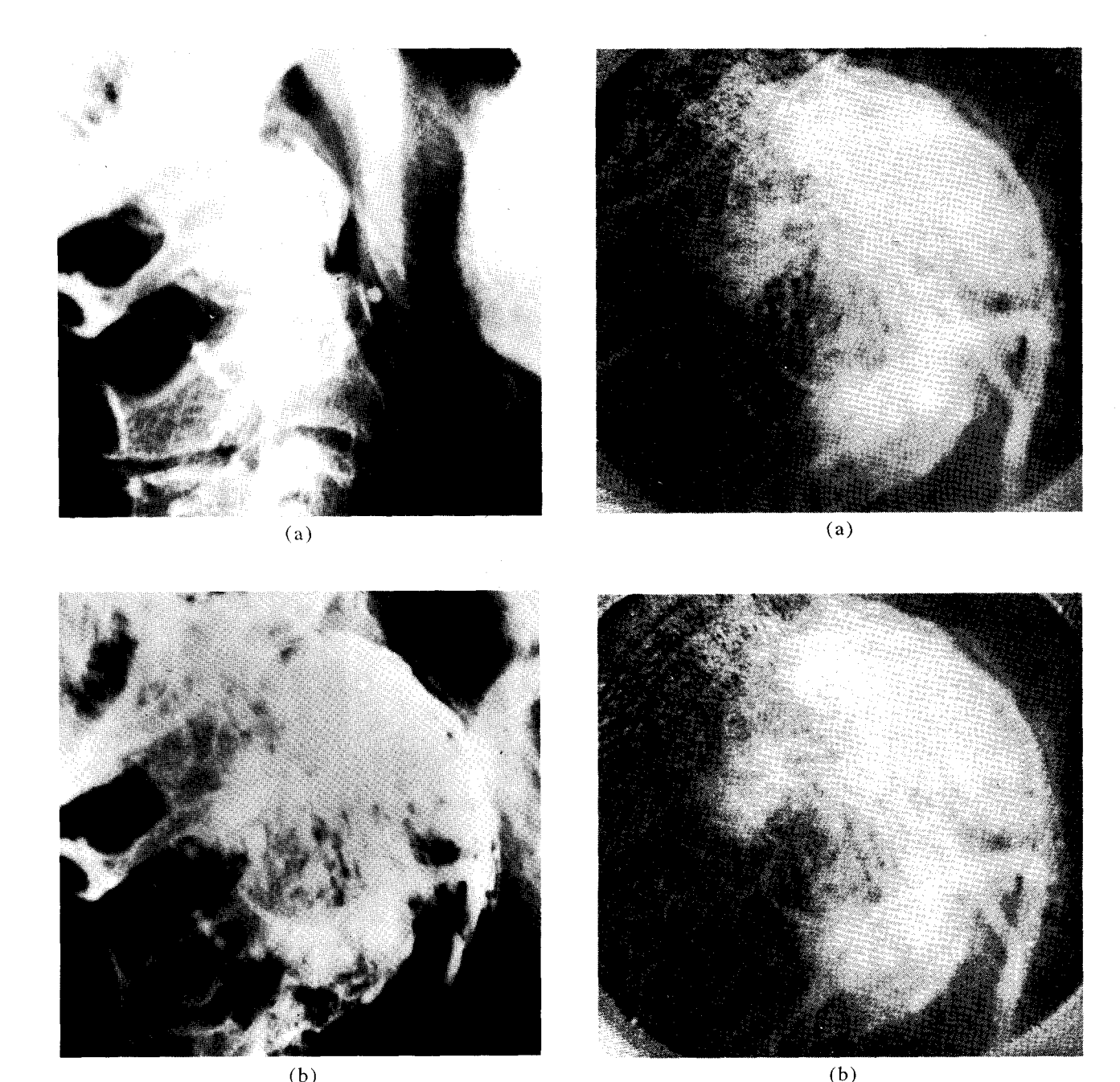


Figure 6 Original images for Case 1; (a) before dye insertion, (b) after dye insertion.

Figure 7 Beta representation for Case 1; (a) prior to registration, (b) subsequent to registration.

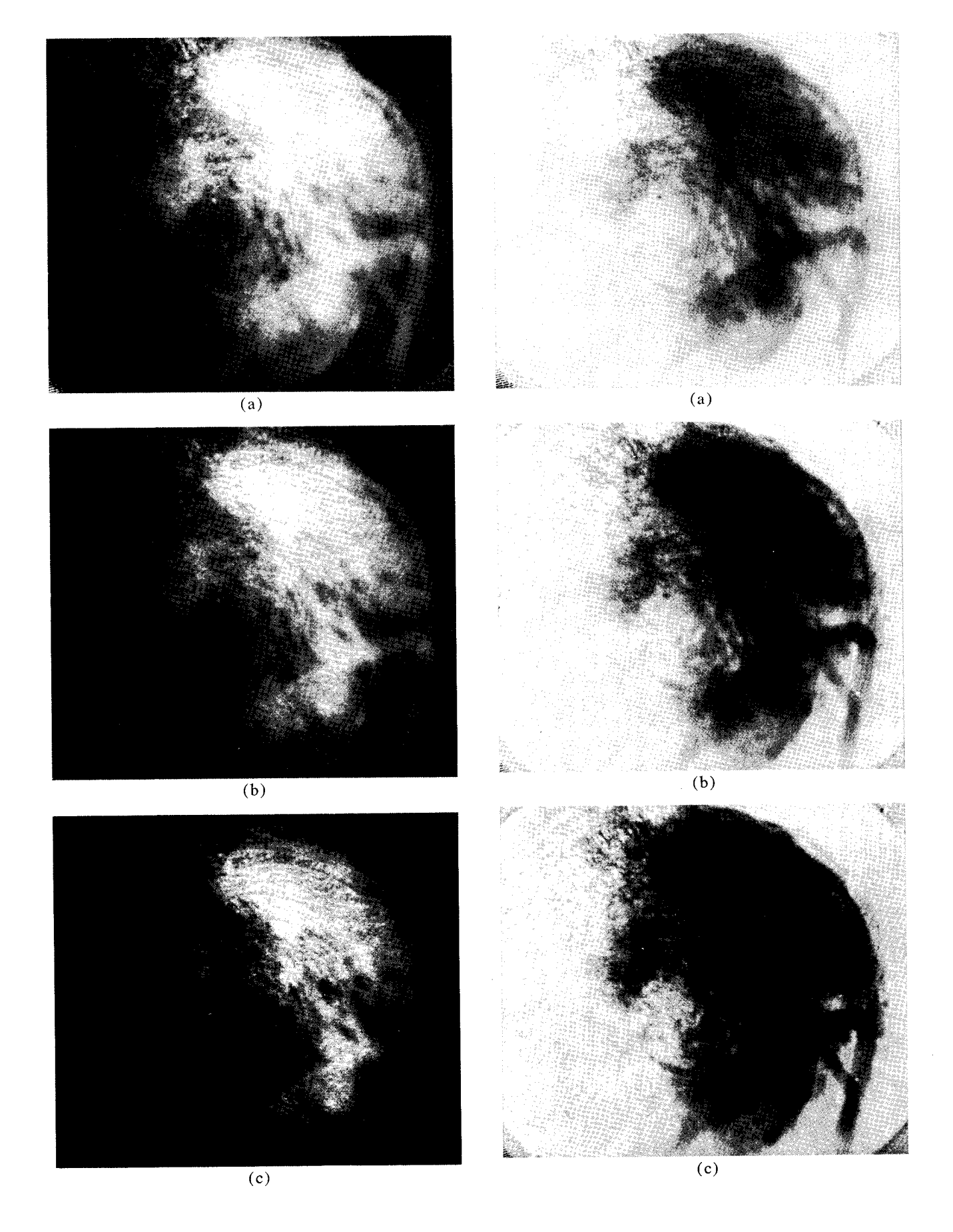
tive" and "negative" artificial images based upon display gamma values (contrast parameters) chosen by the investigators to provide varying levels of contrast. Additionally, the ratio image could be used to compute a $\beta(x, y)$ representation having quantitative usefulness.

The resultant images were recorded on magnetic tape. For immediate inspection, the 1800 system was used to control the production of Polaroid prints showing 512×512 -pixel images. All results shown in this paper

were obtained by this means. However, for full-resolution hard-copy images, it was necessary to print the re-

Figure 8 Digital subtraction with positive contrast parameters for Case 1; (a) $\gamma_c = -1$, (b) $\gamma_c = 2$, (c) $\gamma_c = 3$. (Facing page, left.)

Figure 9 Digital subtraction with negative contrast parameters for Case 1; (a) $\gamma_c = -1$, (b) $\gamma_c = -2$, (c) $\gamma_c = -3$. (Facing page, right.)



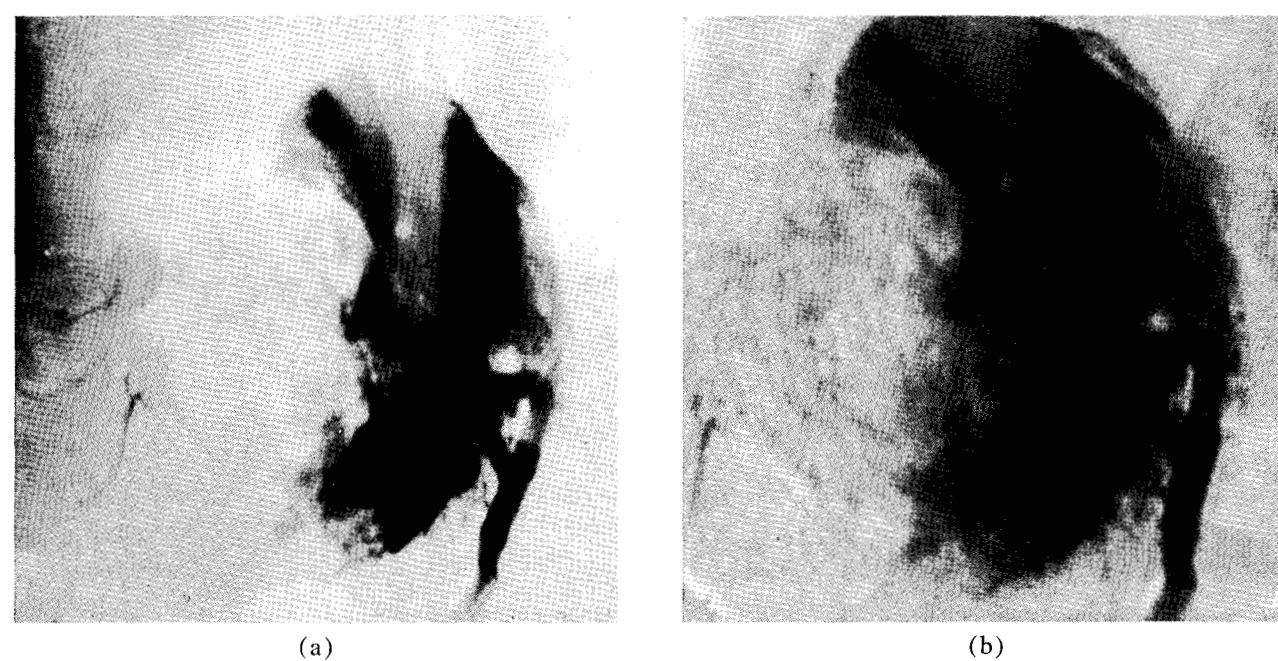


Figure 10 Result of photographic subtraction for Case 1; (a) original photographic result, (b) photographic result after scanning, digitization, and hard-copy playback.

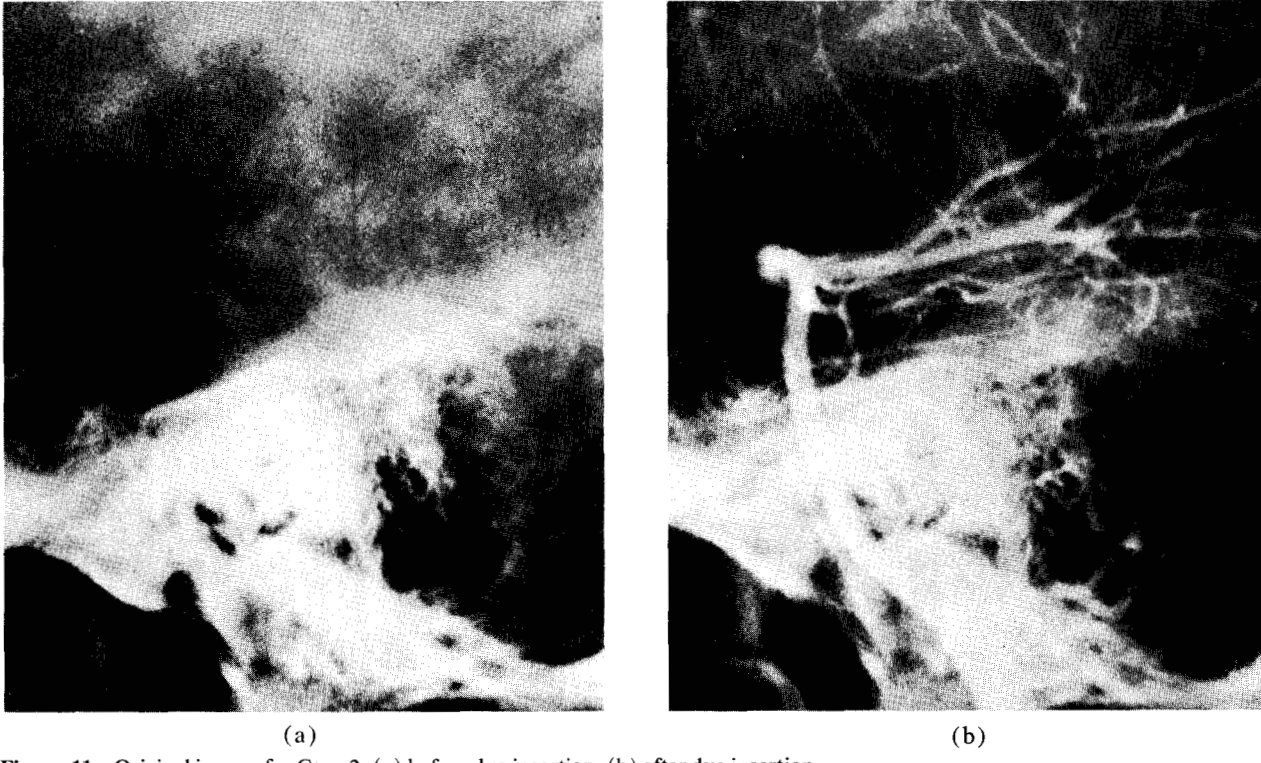


Figure 11 Original images for Case 2; (a) before dye insertion, (b) after dye insertion.

sults on a mechanical drum recorder. In either case, the histogram of each image was used to scale and normalize the range of resultant image values so as to distribute them more fully over the range of film densities available from the recorder. For example, computed image densi-

ties ranging from 0.5 to 1.0 were distributed over the density range of 0.2 to 1.7 available from a recorder. Similarly, computed densities ranging from 0.5 to 7.8 were scaled and normalized to the same 0.2 to 1.7 range. While this approach gives a highly satisfactory visual

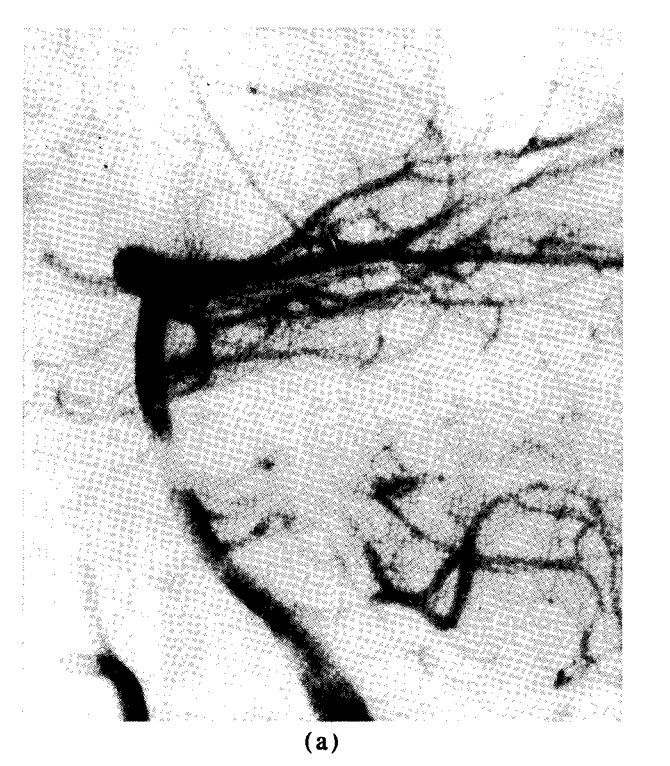




Figure 12 Subtraction for Case 2; (a) photographic, (b) digital, with varied contrast parameters.

result, it is important to note that there no longer exists a 1:1 relationship between a computed transmittance value and the recorded transmittance. To emphasize this discrepancy in the recordings that follow, the values of γ_c used in the computations are referred to as contrast parameter values rather than gamma values.

6. Experimental investigation

A few pairs of images were processed to demonstrate the digital approach to radiographic subtraction. The experimental investigation related to two sets of arteriograms of the head are described in this section of the paper.

The first pair of images (Fig. 6) are angiograms of a vascular tumor behind the angle of the jaw. Similar portions of this set of x-rays were scanned with the image dissector. (The corner structure evident in the following digitally processed images was due to the finite extent of the circular image dissector photocathode.) Both images clearly show a string of spheres (used to partially embolize the tumor) in the lower left quadrant of the pictures. The "before" image shows the upper cervical vertebrae and the angle of the mandible. In the image taken after the radio-opaque medium was injected into the artery supplying the tumor, a large vascular stain is seen to be overlying the bone structure.

Extractions (256×256 pixels) taken from the vicinity of the spheres were used (since they were convenient distinct features) to perform the registration. Typi-

cal TV images obtained during the course of interactive processing have already been shown in Fig. 5. Figure 7 shows the resultant $\beta(x, y)$ representations as computed before and after registration was performed [8]. It is evident that, even with proper registration, some artifact was present. Note the circular structure particularly evident in the upper left quadrant of the image. This problem was traced to hum in the deflection circuits of the image dissector, and the structure introduced is due to incomplete cancellation of the photocathode sensitivity variations.

The final results in terms of digitally generated subtraction images are shown in Fig. 8 for positive values of contrast parameter and in Fig. 9 for negative values. The positive contrast trials attempt to recreate the original exposure as if the background had not been present. The negative contrast cases permit comparison with a print obtained via photographic subtraction. Figure 10 shows the result of photographic second-order subtraction in its original form as well as a version obtained with our recorder after scanning and digitization of the photographic result. An obvious fault present in the photographic result is the presence of jaw structure in the upper central portion of the image. Not only is this background structure significantly suppressed in the digital results, but they more accurately show the true extent of the tumor.

The second pair of images to be described involves the vertebra-basilar circulation in the posterior cranial

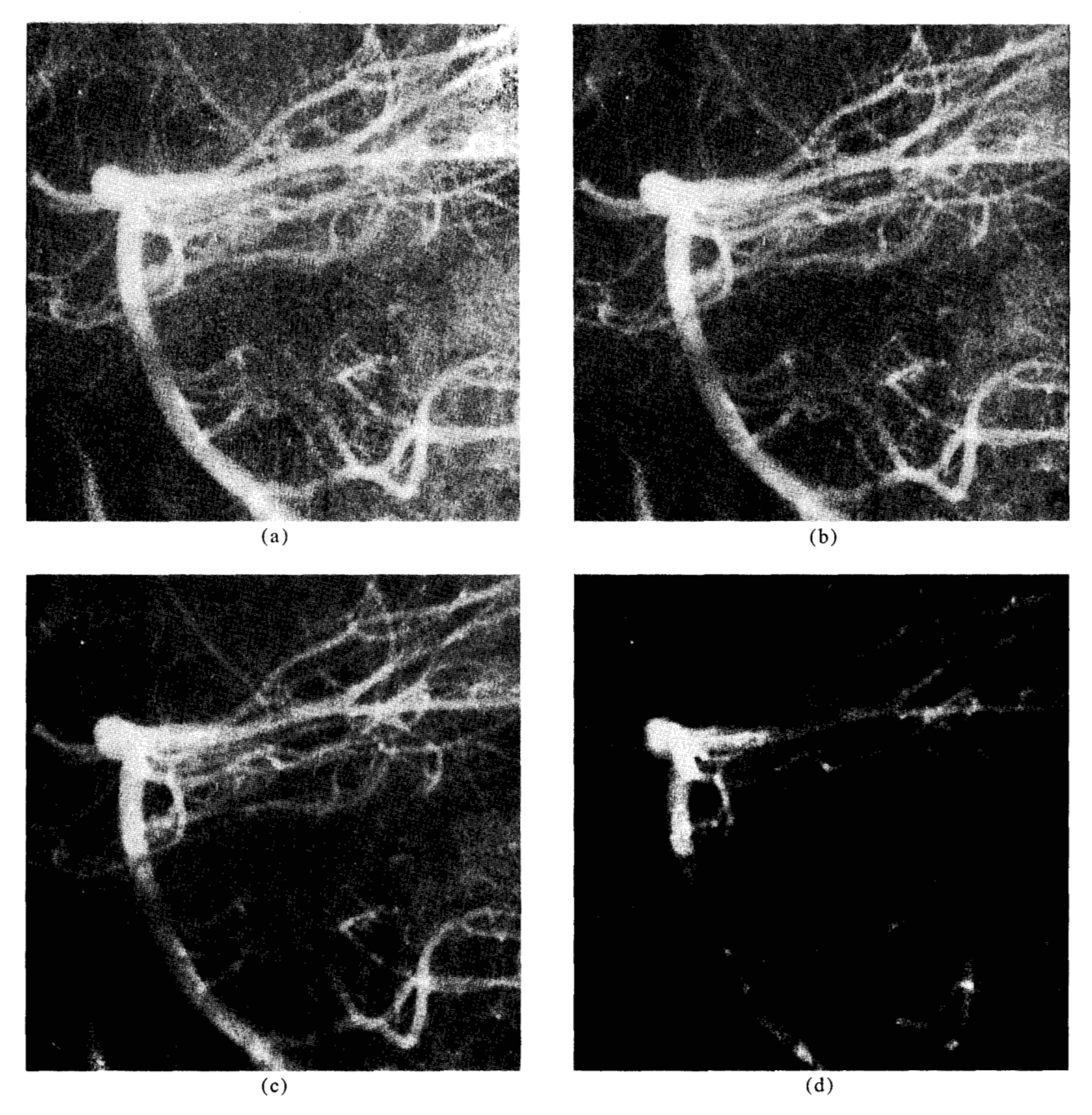


Figure 13 Digital subtraction with positive contrast parameter values for Case 2; (a) $\gamma_c = 1.5$, (b) $\gamma_c = 2.5$, (c) $\gamma_c = 5$, (d) $\gamma_c = 12$.

fossa. The original representations are shown in Fig. 11. The patient has a tumor in the pineal region.

Because of the image dissector hum problem, it was decided to utilize the Optronics drum scanner for this case. These images were scanned at a resolution of $50\mu m$ and a field of 2494×2275 pixels. The processed images were 1024×1024 pixels obtained by averaging groups of four adjacent pixels. The "flat" areas found in the lower left of each image were due to the fact that scan-

ner controls were set to saturate at an image density greater than two. A higher available density setting (three, for example) would have sacrified resolution in the regions of primary interest, which have low density values.

The results obtained in this case for various values of effective positive and negative contrast parameters are shown in Figs. 13 and 14. A photographic subtraction result (again obtained with the second-order technique)

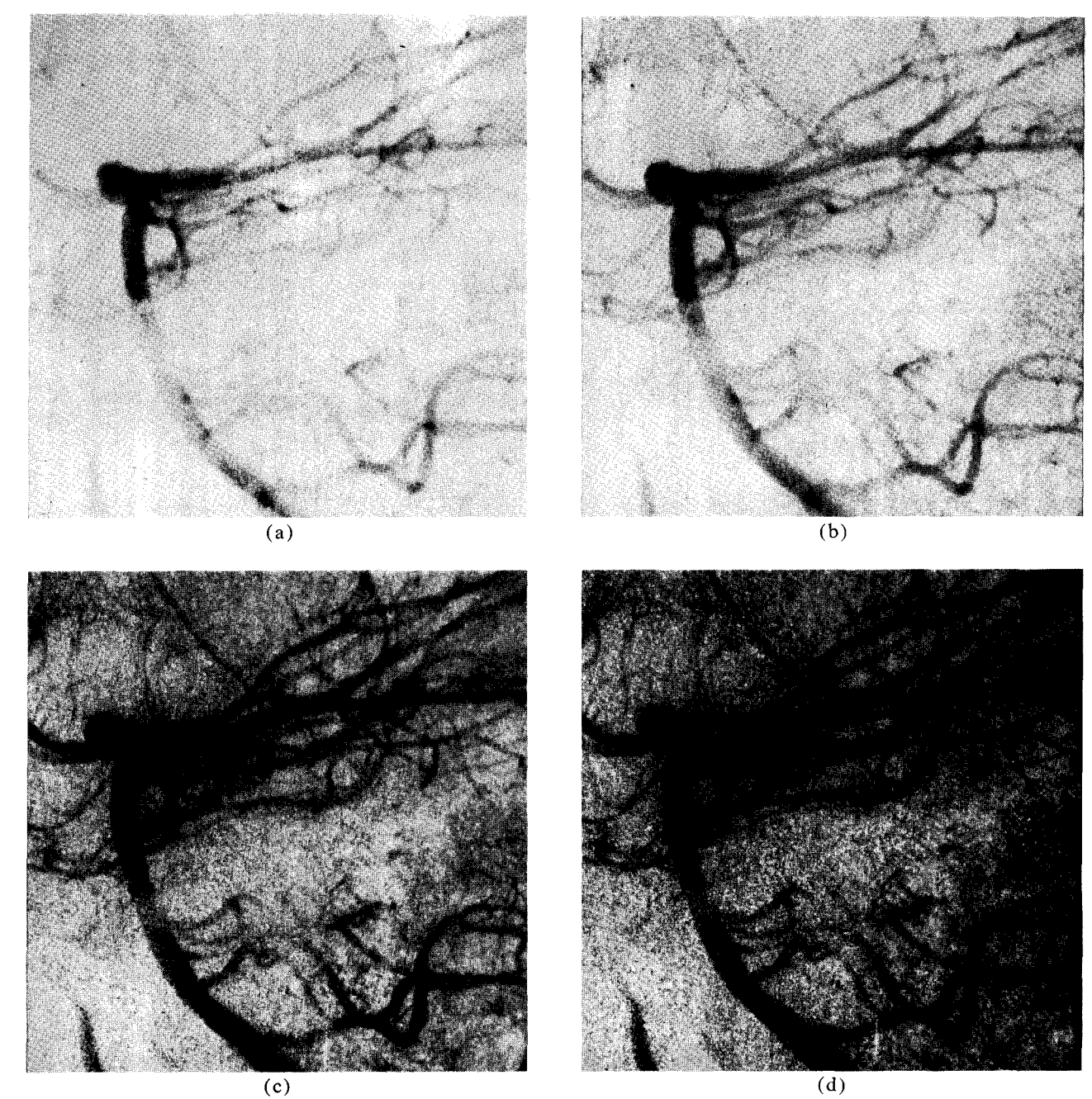


Figure 14 Digital subtraction with negative contrast parameter values for Case 2; (a) $\gamma_e = -1.5$, (b) $\gamma_e = -2.5$, (c) $\gamma_e = -12$, (d) $\gamma_e = -20$.

is shown in Fig. 12(a) for comparison. The result for $\gamma_{\rm e}=-12$ [Fig. 14(c)] is an improvement over the photographic result. The medical result is that the thalamoperforate arteries are well seen and the vessels behind the temporal bone have been markedly enhanced.

Further improvement is possible and convenient to realize digitally. Examination of the results shown in Fig. 14 indicates that the use of a fixed-contrast parameter can provide a good presentation over only a portion

of each image. For example, $\gamma_{\rm c}=-20$ provided best perception of detail in the high background region while sacrificing perception in some areas of low background regions. It is in this type of situation where automatic contrast adjustment using the background exposure as a control function can prove useful. The result of such an enhancement implementation is shown in Fig. 12(b), where the contrast parameter was varied automatically and spatially between the extremes of -5 and -20.

References and notes

- 1. B. G. Ziedses des Plantes, Subtraktion, Georg Thieme Verlag, Stuttgart, 1961.
- R. H. Selzer, "Digital Computer Processing of X-ray Photographs," California Institute of Technology JPL Technical Report #32-1028, Nov. 15, 1966.
- 3. To the extent that the characteristic is linear, the formula, $\beta(x,y)=(1/\gamma_x) \ln \left[T_a(x,y)/T_b(x,y)\right]$, involving directly measured transmittances and characteristic curve slope γ_x applies.
- 4. W. Hanafee and P. Stout, "Subtraction Technic," *Radiology* 79, 658 (1962).
- 5. J. C. Stevens and S. S. Stevens, "Brightness Function: Effects of Adaptation," J. Opt. Soc. Am. 63, 375 (1963).
- N. M. Herbst and P. M. Will, "An Experimental Laboratory for Pattern Recognition and Signal Processing," Comm. ACM 15, 231 (1972).

- 7. D. I. Barnea and H. F. Silverman, "A Class of Algorithms for Fast Digital Image Registration," *IEEE Trans. Computers* C-21, 179 (1972).
- 8. The resolution of all digitally processed images shown corresponds to 512 × 512 pixels although scanning and final processing normally was at twice this resolution.

Received June 13, 1972

C. K. Chow and K. E. Niebuhr are located at the IBM Thomas J. Watson Research Center, Yorktown Heights, New York 10598. S. K. Hilal is associated with the the Neurological Institute of the Columbia-Presbyterian Medical Center, New York, New York 10032.